EGTRIB Journal
JOURNAL OF
THE EGYPTIAN SOCIETY OF TRIBOLOGY
VOLUME 22, No. 3, July 2025, pp. 80 - 97 **ISSN 2090 - 5882**
(Received May 19. 2025, Accepted in final form June 23. 2025) **jest.journals.ekb.eg**

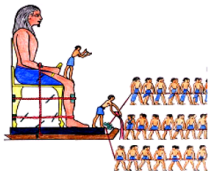

OPTIMIZATION OF GRAPHENE-BASED NANOFILLER COMBINATIONS IN PMMA DENTAL COMPOSITES USING TAGUCHI APPROACH

Sinossi M. I.[1], Abdu H. M.[2], Ameer A. K.[2], Hussein H.[3]

[1]Mechanical Design and Production Department, Faculty of Engineering, Beni-Suef University,
[2]Production Engineering and Mechanical Design Department, Faculty of Engineering, Minia University, 61111 El-Minia,
[3]Department of Mechanical Engineering, Higher Technological Institute, 10th of Ramadan City, EGYPT.

ABSTRACT
This current work carries out an extensive analysis of the optimization of poly (methyl methacrylate) (PMMA) dental composites utilizing the Taguchi technique. The PMMA composites have been enriched using multiple graphene-based nanofillers. A mixed-level L16 orthogonal array was developed to examine the impact of three key parameters, kind of filler, loading level, and curing process, on tribological and mechanical attributes. The outcomes of the study responses comprised the coefficient of friction (COF), weight loss (WL), and hardness (H). It can indicate that the curing process exerted the biggest impact on hardness (33.75%), succeeded by filler type (22.09%) and loading level (10.25%). The outcomes indicate that the most suitable conditions for decreasing COF and WL and maximum hardness were identified as graphene filler, 0.5 N loading, and heat curing. The RSM models revealed a good prediction accuracy, with correlation values (R^2) of 0.9468, 0.9725, and 0.9989 for COF, WL, and hardness, respectively. Multi-objective optimization applying desire function analysis proved these settings as the most successful. The merger of Taguchi and RSM techniques gives a solid approach for optimizing nanocomposite features in advanced dental applications.

KEYWORDS
PMMA composites, graphene, friction and wear rate, optimization.

INTRODUCTION
Polymeric materials are appreciated to serve distinct functions in various marketplaces. This contributes to constant advancement and innovation in their benefits through extensive research plans, [1 - 4]. Polymethyl methacrylate (PMMA) is a thermoplastic polymer recognized for its transparency, rigidity, and durability, rendering it extremely useful across multiple sectors. [5, 6]. PMMA is commonly employed in the production of shatter-resistant windows, LED lighting components,

automotive windows, motorcycle windshields, and optical lenses. In addition, it finds frequent use in dental applications such as cavity fillings, denture bases, and bone cement. These uses can be attributed to its excellent biocompatibility and formability, as well as its favourable aesthetic qualities, [5, 7]. Consequently, PMMA is currently ranks among the most utilized substances in denture fabricate, [8, 9]. Dental acrylic resins are usually made of two initial constituents: a powder ingredient, known as a modified version of PMMA, and a liquid ingredient, methyl methacrylate, that functions as the monomer or solvent. PMMA, an acrylic-based resin, is commonly used in dental applications and is manufactured by the polymerization of methyl methacrylate (MMA) monomers [10]. The use of alginate as a stabilizer is technically sufficient to produce spherical PMMA microparticles, whereas gelatin stabilizers tend to produce finer particles, [11 - 13]. Moreover, PMMA resin exhibits excellent compressive and tribological qualities, these attributes alone are inadequate to fulfil the standards for wear resistance, hardness, and comprehensive mechanical strength. Therefore, unaltered PMMA is often viewed as inadequate for dental settings.

ZrO_2, Al_2O_3, SiO_2, and other metal oxides were adopted as modifiers of PMMA matrices that were produced through a variety of techniques, [14]. The fillers are primarily used to enhance the mechanical properties of the system. Furthermore, the curing method and duration have been shown to significantly influence the hardness and friction coefficient of PMMA matrices reinforced with TiO_2 nanoparticles, [15, 16]. The friction coefficient gradually decreases with increasing TiO_2 content. The friction coefficient and wear rate are further reduced by the gradual addition of TiO_2/ZnO nanoparticles, [17] . It has also been discovered that adding ZnO nanotubes improves the composite's thermal performance and flexural strength, [18]. Furthermore, efforts were investigated to incorporate both natural and synthetic fibers to reinforce PMMA monomers, [19]. Based on its outstanding biocompatibility and high adherence to PMMA, fiberglass has proven to be a useful support for dental composites, [20]. The physical, chemical, thermal, and biocompatible properties of PMMA/glass fiber composites as well as the causes of denture fractures have been the topic of various study, [21]. Both Barium glass particles and silanated glass fibers were successfully employed as reinforcing components in dental composites. Combination fillers greatly increase fracture toughness and decrease polymerization shrinkage, in line with experimental data, [22]. In another study, the reinforcement system included nylon-6 dissolved in hexafluoro isopropanol (10 wt.%) combined with multi-walled carbon nanotubes (MWCNTs) at loadings of 0.5% and 1.5%, aiming to improve the flexural strength of PMMA-based dental resins, [23]. Results showed that both wear rate and friction coefficient decreased in hot- and cold-cured PMMA/MWCNT composites, while hardness increased in the hot-cured systems with rising MWCNT concentration, [24]. Thermogravimetric analysis (TGA) confirmed uniform dispersion of MWCNTs within the PMMA matrix. The fatigue resistance, flexural performance, and resilience of PMMA/MWCNT composites exhibit a good reaction better than the commercial PMMA, [25].

The resulting PMMA composites exhibited improved mechanical and physical performance [26]. The addition of nanographene (NG) and hybrid fillers like SiO_2–

TiO_2 to PMMA denture base resins improved both tribological performance and hardness. Furthermore, the influence of the durability of the PMMA/NG composite with SiO_2/TiO_2 increased by 18% when compared to the free PMMA structure, [27]. Rheological parameters, including viscosity, absorption coefficient, and specific viscosity, were examined and indicated significant gains with the inclusion of graphene oxide GO. The results revealed that viscosity rose by up to 57% compared to standard fillers. The inhibitory region for mite-causing bacteria, such as Enterococcus faecalis and Staphylococcus aureus, was further enhanced by up to 46% with the incorporation of GO, [28]. Taguchi's experiment (DOE) technique is particularly valuable in polymer research, where multiple variables—such as filler type, content, curing temperature, and curing method—interact to influence mechanical, thermal, and tribological performance [29], [30]. Researchers have successfully applied Taguchi's design of experiments (DOE) to enhance the tensile strength, stiffness, and wear resistance of thermoplastic and thermosetting matrices reinforced with fibers, nanoparticles, or hybrid fillers, [31, 32]. This method employs orthogonal arrays systematically assessing parameter combinations, resulting in optimal composite formulations, [33, 34]. Moreover, Taguchi's signal-to-noise (S/N) analysis enhances material uniformity and performance dependability under fluctuating workloads. Current studies have expanded this method to encompass polymeric composites utilized in dentistry and biomedicine, where precise mechanical tuning is essential.

This study proposes a framework for enhancing the mechanical attributes of polymethyl methacrylate (PMMA) dental composites through the strategic incorporation of graphene-based nanofillers. Using a Taguchi design of experiments, different filler formulations—graphene (GN), GN + SiO_2, GN + TiO_2, and GN + SiO_2 + TiO_2—were evaluated at different loading levels and processing methods. The content level that maximizes hardness and wear resistance was the aim. The experimental design utilizes an orthogonal L16 matrix to minimize testing while capturing the interactions of key variables. Microscopic and mechanical analyses, including SEM and hardness testing, confirm the validity of the results. These findings are expected to contribute to the development of high-performance and durable dental materials. This approach aligns with the ongoing demand for advanced and functional biomaterials in restorative dentistry.

EXPERIMENTAL

Materials

Poly (methyl methacrylate)-based acrylic resin is widely utilized in dental restorations due to its easy handling and appealing cosmetic properties. PMMA components were supplied from Egypt's Acrostone Dental and Medical Supplies. Methyl methacrylate (MMA), an insoluble monomer, and modified PMMA powder make up a PMMA substance. Nano-fillers such as graphene (GN), silicon dioxide (SiO_2), and titanium dioxide (TiO_2) are used alone or in combination for strengthening. All the nano-additives were purchased from US Research Nanomaterials, Inc. in the United States. Graphene nanoparticles were provided as black flakes with lateral dimensions ranging from 2 to 10 µm and an average thickness of less than 5 nm. SiO_2 and TiO_2

were provided as white spherical particles with average sizes of 45–60 nm and specific surface areas of approximately 35 m^2/g, with respective densities of 2200 kg/m^3 and 3900 kg/m^3.

Sample Preparation

The monomer-to-polymer mixing ratio was maintained at 1:2 (liquid to powder), consistent with standard dental resin preparation procedures. The polymerization process began by blending PMMA powder with MMA liquid, followed by the addition of nano-fillers according to the experimental matrix designed using the Taguchi method. Each formulation contained one of the following filler systems: GN, GN + SiO_2, GN + TiO_2, or GN + SiO_2 + TiO_2, at varying weight fractions of 0.25%, 0.5%, 0.75%, and 1.0%. Subsequently being mixed into the resin matrix, ingredients were evenly distributed in MMA utilizing magnetic stirring and ultrasonic agitation. For an interval of ten minutes, the filler-resin mixtures were physically agitated at 200 rpm while being held at room temperature (30 °C and 55% relative humidity). Viscosity rose as polymerization went on, forming a homogeneous paste. Following being packed into cylindrical molds measured 8 mm in diameter by 25 mm in height, the paste was squeezed for 45 minutes at a pressure of 10 bar. However, to the experimental design, two curing techniques—cold cure and heat cure—were performed, based on the formulation. The substance of filler and filling amount were utilized to identify each sample (e.g., GN-025, GN+SiO_2-050, GN+SiO_2+TiO_2-100, etc.). The setting up methods for the PMMA nanocomposites enhanced with hybrid nano-fillers are shown in Fig. 1.

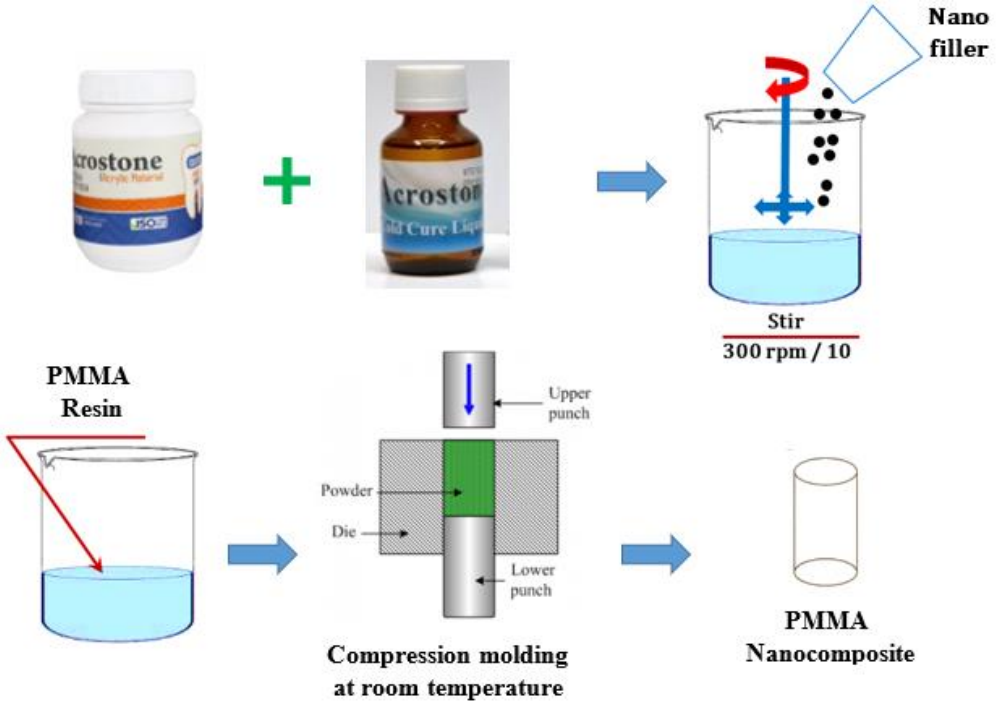

Fig. 1. Schematic representation of the PMMA composites' setting up.

Evaluation and Characterization

To investigate and evaluate the different mechanical performance of PMMA nanocomposite, samples are made. In accordance with ASTM standard D2240, samples are examined and their hardness attributes measured using the durometer Shore D apparatus. After testing the hardness value five times across the sample surface, the average value was calculated. Standard errors were included in the average statistics.

In accordance with ASTM standard G99-95, a reciprocating pin-on-disk tribometer was used to conduct the tribological attributes. The samples are examined in a room climate with a temperature of 30°C and a relative humidity of 55%, as well as dry contact settings. Stainless steel, the disk's material, was chosen to meet the real standards. The investigations were carried out at a constant linear velocity of 0.6 m/s while applying weights of 6, 8, 10, and 12 N. The difference in weight between each sample's original and final weights was used to calculate wear findings. The electronic microscope (OLYMPUS BX53M, USA) and scanning electron microscopy (SEM) microscope (JCM-6000Plus; JEOL, Tokyo, Japan) were utilized to examine the worn sides. To prepare the sample surfaces for SEM photography, they are first cleaned by washing and then completely dried with air. Finally, a thin layer of platinum is applied to the surfaces.

Design of experiments

Taguchi method has been recommended to limit the influence of uncontrollable factors, which has been considered as a mathematical strategy, that minimizes the number of experiments. Taguchi finds minor variables quickly by building orthogonal arrays and matching multiple variables. Taguchi method has been utilized to analyze the data and identify the ideal conditions for the Coefficient of friction. A set of experiments on different levels of parameters has been created and carried out based on Taguchi methodology. An experimental design called the L16 orthogonal array (Mixed level design 4^2 2^1) has been constructed using Minitab software version 21.4. To identify the most affecting factors and their interactions, the operational parameters have been examined. Three independent input variables— Type of Filler (X_1), Loading (X_2), and Curing Method (X_3)—have been selected. The selected variables have been converted into dimensionless factors X_1, X_2, and X_3 (see Table 1). Only 16 experiments to determine the optimal variable levels, table (1) shows first design and table (2) The Experimental results of all responses are practically required to be performed instead of 256 ($4^4 = 256$) through the examination of three variables at four levels. Table 2 shows four replications for each Experimental design.

Table 1 Levels of Process Parameters

Input Parameter	Unit	Symbol	Level			
			1	2	3	4
Type of Filler		X_1	GN	GN + SiO_2	GN + TiO_2	GN + SiO_2+ TiO_2
Loading	N	X_2	0.25	0.5	0.75	1.0
Curing Method		X_3	Cold Cure		Heat Cure	

Table 2 The Experimental design for PMMA composites

Exp. No	Type of Filler (X_1)	Loading level (X_2)	Curing Method (X_3)
1	GN	0.25	Cold cure
2	GN	0.5	Cold cure
3	GN	0.75	Heat cure
4	GN	1.0	Heat cure
5	GN + SiO_2	0.25	Cold cure
6	GN + SiO_2	0.5	Cold cure
7	GN + SiO_2	0.75	Heat cure
8	GN + SiO_2	1.0	Heat cure
9	GN + TiO_2	0.25	Heat cure
10	GN + TiO_2	0.5	Heat cure
11	GN + TiO_2	0.75	Cold cure
12	GN + TiO_2	1.0	Cold cure
13	GN + SiO_2+ TiO_2	0.25	Heat cure
14	GN + SiO_2+ TiO_2	0.5	Heat cure
15	GN + SiO_2+ TiO_2	0.75	Cold cure
16	GN + SiO_2+ TiO_2	1.0	Cold cure

Taguchi Optimization of the Coefficient of friction, weight loss and hardness

In 16 experimental operates, these monitoring parameters were examined at Multi level design [4^2 2^1] according to L16 Taguchi orthogonal array, as demonstrated in Table 3. The planned trials were carried out at random to account for the impacts of noise elements that were not considered in the experimental design mesh of the weight loss and coefficient of friction. The coefficient of friction, weight loss, and the S/N ratio "Smaller is better (SIB)" are the optimization parameters (response) according to Equation 1. When the variables' response is denoted by y and the number of experiments by n.

$$S/N = -10\ Log\ (\sum \frac{Y^2}{n}) \qquad [1]$$

Table 3 The Structure matrix of the elements and their levels applied for Taguchi assessment utilizing the S/N ratio of COF, WL and Hardness

Exp. No	Type of Filler (X_1)	Loading level (X_2)	Curing Method (X_3)	CoF	WL	H
1	GN	0.25	Cold cure	0.45	0.0026	82.1
2	GN	0.5	Cold cure	0.41	0.002	81.9
3	GN	0.75	Heat cure	0.42	0.0022	82.2
4	GN	1.0	Heat cure	0.44	0.0025	82.1
5	GN + SiO_2	0.25	Cold cure	0.47	0.0028	82.1
6	GN + SiO_2	0.5	Cold cure	0.46	0.006	82.7
7	GN + SiO_2	0.75	Heat cure	0.4	0.0022	83.1
8	GN + SiO_2	1.0	Heat cure	0.43	0.0021	83
9	GN + TiO_2	0.25	Heat cure	0.44	0.0028	82.2

10	GN + TiO_2	0.5	Heat cure	0.4	0.0023	81.9
11	GN + TiO_2	0.75	Cold cure	0.49	0.0032	82.5
12	GN + TiO_2	1.0	Cold cure	0.51	0.0038	82.4
13	GN + SiO_2+ TiO_2	0.25	Heat cure	0.46	0.0026	84.1
14	GN + SiO_2+ TiO_2	0.5	Heat cure	0.42	0.0023	84.9
15	GN + SiO_2+ TiO_2	0.75	Cold cure	0.45	0.0025	83.2
16	GN + SiO_2+ TiO_2	1.0	Cold cure	0.46	0.0027	83.1

Therefore, fewer tests were conducted, and both time and expense savings were realized. Thus, depending on the goal of the investigations, both the mean effect and the signal-to-noise ratio have been used in quantifiable levels of qualitative features. Equation 2, where y is the hardness response of the factors listed in the previous table and n is the number of trials. For the purpose of including the impacts of noise components that were not considered in the experimental design matrix of the coefficient of friction, weight loss, and hardness, experiments were carried out at random.

$$S/N = -10\ Log\ (\frac{1}{n}\sum\frac{1}{Y^2}) \quad [2]$$

Statistical analysis

Statistics of the friction summarize the S/N ratio's reaction results regarding the friction coefficient and contact weight loss as determined by the Taguchi technique. The S/N ratio for each control parameter at various values is described. The average experimental findings for each factor at each level are denoted by the numerical designations 1, 2, and 3. Additionally, 'Delta' denotes the difference between the greatest and lowest S/N ratios for each control factor throughout the three levels, providing information on the main and secondary degrees of impact for each factor in the experimental results. The friction coefficient's S/N ratio at the loading levels is 0.732, the highest of the three S/N ratio values, as revealed by the results in Table 5.

Table 5 S/N ratio response for COF

Friction coefficient (COF)			
Level	Type of Filler	Loading	Curing Method
1	7.337	6.842	6.714
2	7.148	7.496	7.416
3	6.784	7.156	-
4	6.990	6.764	-
Delta	0.553	0.732	0.702
Rank	3	1	2

Table 6 S/N ratio response for WL

Weight Loss (WL)			
Level	Type of Filler	Loading	Curing Method
1	52.72	51.38	50.36
2	50.55	50.99	52.52
3	50.53	52.06	-
4	51.97	51.34	-

Delta	**2.19**	**1.07**	**2.16**
Rank	**1**	**3**	**2**

Table 7 S/N ratio response for Hardness

Hardness			
Level	**Type of Filler**	**Loading**	**Curing Method**
1	**38.28**	**38.34**	**38.33**
2	**38.35**	**38.36**	**38.37**
3	**38.30**	**38.36**	**-**
4	**38.47**	**38.34**	**-**
Delta	**0.18**	**0.02**	**0.05**
Rank	**1**	**3**	**2**

Furthermore, the S/N ratio has a minimum value of 0.553 at the type of filler levels. Furthermore, transitioning from cold to heat cure reveals a significant variation in the friction coefficient. This is exhibited that loading is the primary influencing element, while the curing procedure is of lesser importance (refer to Table 5). Consequently, the subsequent ordering of the components influencing the friction coefficient is as follows: loading > curing technique > filler type, while for weight loss, the order is: fillers type > curing technique > load (refer to Table 6). It is evident from the S/N ratio analysis that loading and its curing strategy have significant effects on the friction coefficient, whereas filler type and curing strategy have a significant impact on weight loss. S/N ratios ought to be continuously maximized under ideal circumstances. Thus, the S/N ratios and levels necessary to achieve the optimal friction coefficient value are specified as follows: Typer of filler (GN, S/N = 7.336), load (0.5 N, S/N = 7.495), and curing method (Heat cure, S/N = 7.415). Similarly, for Weight loss, the optimal parameter combination comprises Typer of filler (GN, S/N = 52.718), load (0.75 N, S/N = 52.06), and curing method (Heat cure, S/N = 52.523).

Figures 2 and 3 provide a visual representation of the level values of control variables for these attributes as displayed in Tables 5 and 6. These visual aids make it simple to identify the ideal settings for reducing or improving the friction coefficient and weight loss. The outcomes from the S/N ratio analysis are summarized in Table 7, where the filler type is the parameter with the highest ranking for hardness. The loading parameter, on the other hand, is rated third for both outputs, indicating that it has the least effect on hardness. The optimal combination of parameter hardness is represented by bold values, whereas delta values are used to determine parameter ranking according to Table 7.

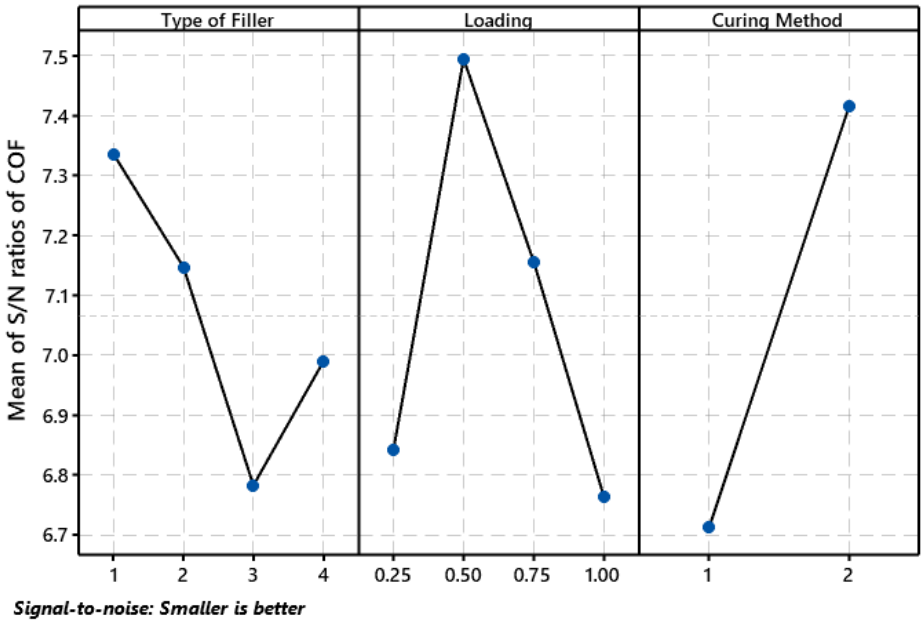

Fig. 2 Impact of control parameter on average S/N ratio for COF.

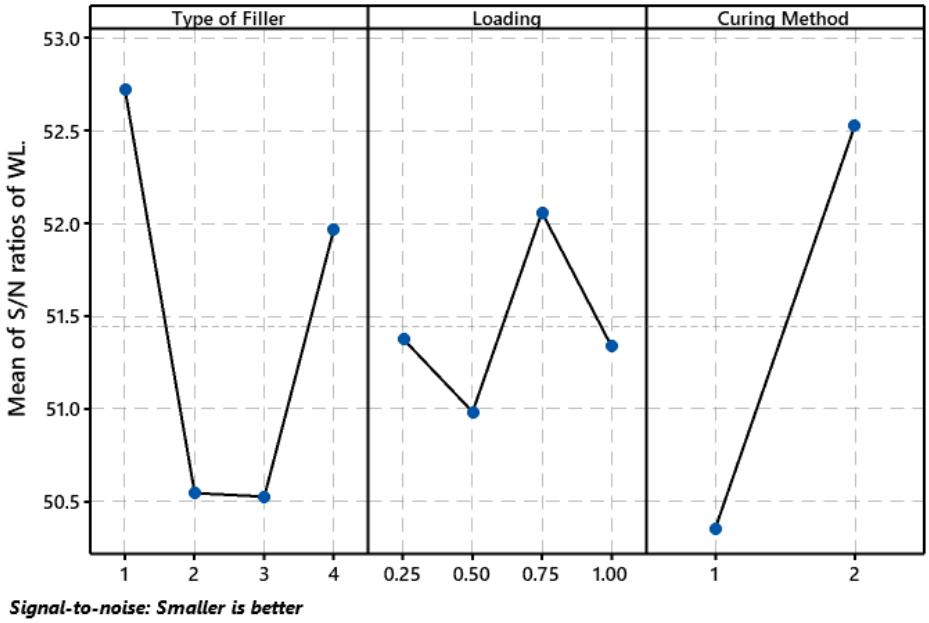

Fig. 3 Impact of control parameter on average S/N ratio for WL.

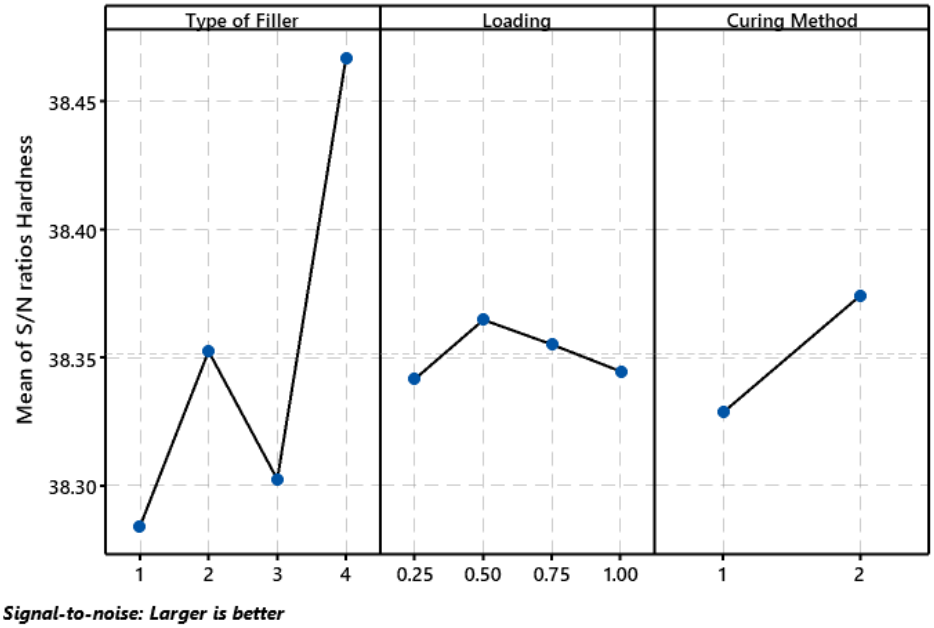

Fig. 4 Impact of control parameter on average S/N ratio for Hardness.

Analysis of Variance, ANOVA, is a statistical method used to evaluate the unique interactions between each control variable in a particular design of experiments. The impacts of filler type, loading, and curing process on the friction coefficient and weight loss were examined and evaluated in this study employing ANOVA. Indeed, a 95% confidence level and a 5% significant level were used for the study. Comparing the F values for each control factor in an ANOVA is necessary to determine the importance of the control variables [35]. Tables 8, 9, and 10 provide the ANOVA findings for the friction coefficient, weight loss, and hardness of contact, appropriately.

Table. 8 Analysis of Variance for friction coefficient

Source	DF	Seq SS	Adj SS	Adj MS	F-Value	P-Value	Contribution
Type of Filler	3	0.0851	0.0851	0.0284	23.667	10.21	74.85 %
Loading	3	0.0019	0.0019	0.0001	0.083	0.45	1.67%
Curing Method	1	0.0091	0.0091	0.0091	7.583	3.04	8.01 %
Error	8	0.0176	0.0176	0.0012			15.47 %
Total	15	0.1137					100.00%

[a] Df: degrees of freedom; SS: sum of squares; MS: Variance; *P*: percent contribution. * Pooled, Tabulated *F*- ratio at 99% and 95% confidence level: $F0.01, 3, 8 = 7.59$, $F_{0.05, 3, 8} = 4.07$, $F_{0.05, 1, 8} = 5.32$

Table. 9 Analysis of Variance for weight loss

Source	DF	Seq SS	Adj SS	Adj MS	F-Value	P-Value	Contribution
Type of Filler	3	0.6616	0.6616	0.2205	1.69	0.363	12.22%
Loading	3	1.7368	1.7368	0.5789	4.44	0.146	32.09%
Curing Method	1	1.9718	1.9718	1.9718	15.13	0.004	36.43%
Error	8	1.0427	1.0427	0.13033			19.26 %
Total	15	5.4129					100.00%

[a] Df: degrees of freedom; SS: sum of squares; MS: Variance; *P*: percent contribution. * Pooled, Tabulated *F*- ratio at 99% confidence level: $F_{0.01, 3, 8} = 7.59$, $F_{0.01, 1, 8} = 11.26$

Table. 10 Analysis of Variance for hardness

Source	DF	Seq SS	Adj SS	Adj MS	F-Value	P-Value	Contribution
Type of Filler	3	18.131	6.044	18.131	1.73	1.02	22.09 %
Loading	3	8.413	2.804	8.413	0.80	0.14	10.25%
Curing Method	1	27.704	27.704	27.704	7.94	3.29	33.75 %
Error	8	27.844	3.4905	27.844			33.91 %
Total	15	82.092					100.00%

[a] Df: degrees of freedom; SS: sum of squares; MS: Variance; *P*: percent contribution. * Pooled, Tabulated *F*- ratio at 95% confidence level: $F_{0.05, 3, 8} = 4.07$, $F_{0.05, 1, 8} = 5.32$

ANOVA results for the friction coefficient (refer to Table 8) show that curing method has the most factor effect on COF at contributes 36.43 % and the loading is the second factor effect at contributes 32.09 %. There are three degrees of statistical significance: 90%, 95%, and 99% for the Curing Method and 90% and 95% for the Loading Method. On the other hand, Table 8 shows that curing methods have the most factor effect on weight loss at contributes 33.75 % and Type of Filler is the second factor effect at contributes 22.09 %. The Curing Method is statistically significant at 90%, 95% confidence levels. ANOVA results for the friction coefficient (refer to Table 10) show that type of filler is the most factor on hardness at contributes 74.85 % and the curing method is the second factor effect at contributes 8.01 %. Table 11 and figure 1 show how different operating factors affect the COF S/N ratio and weight loss (refer to Table 11). It is obvious that the Type of Filler at level 1 (GN), Loading at level 2 (0.5 N), and Curing Method at level 2 (Heat cure) are the ideal values for various aspects of control to accomplish reducing COF. Table 12 and Fig. 2 demonstrate the influence of different operating factors on the S/N ratio, leading to up the weight loss. It is apparent that the Type of Filler at level 1 (GN), Loading at level 3 (0.75 N) and Curing Method at level 3 (Heat cure) are ideal settings for different control parameters to achieve minimal WL.

Table 11. Effect of factors on S/N (COF)[a]

Symbol	Factors	S/N ratios (dB)			
		L 1	L 2	L 3	L 4
X_1	Type of Filler	GN[a]	GN + SiO_2	GN + TiO_2	GN + SiO_2+ TiO_2
X_2	Loading	0.25	0.5[a]	0.75	1
X_3	Curing Method	Cold cure	Heat cure [a]		

Table 12. Effect of factors on S/N (WL)[a]

Symbol	Factors	S/N ratios (dB)			
		L 1	L 2	L 3	L 4
X_1	Type of Filler	GN[a]	GN + SiO_2	GN + TiO_2	GN + SiO_2+ TiO_2
X_2	Loading	0.25	0.5	0.75 [a]	1
X_3	Curing Method	Cold cure	Heat cure [a]		

Table 13. Effect of factors on S/N (Hardness)[a]

Symbol	Factors	S/N ratios (dB)			
		L 1	L 2	L 3	L 4
X_1	Type of Filler	GN	GN + SiO_2	GN + TiO_2	GN + SiO_2+ TiO_2 [a]
X_2	Loading	0.25	0.5[a]	0.75	1
X_3	Curing Method	Cold cure	Heat cure [a]		
a Optimum level					

It can be concluded from Table 13 and Figure 3 that the following parameters work well together to produce the highest hardness: GN + SiO_2+ TiO_2 filler type (level 4), 0.5 N loading (level 2), and heat cure (level 2) curing strategy. The response optimizer function for COF and WL based on S/N ratio is used to place the optimal circumstances, as demonstrated in Fig. 4. The optimum drawn conditions of COF are type of filler GN, loading 0.5 N and Curing method of heat cure. The optimization achieved a desirability score of 0.856, corresponding to a minimum predicted COF of 7.6549 (Fig. 5 a). While the optimum drawn conditions of WL are type of filler GN, loading 0.75 N and Curing method of heat cure. The optimization achieved a desirability score of 0.119, corresponding to a minimum predicted WL of 52.9115 (Fig. 5 b).

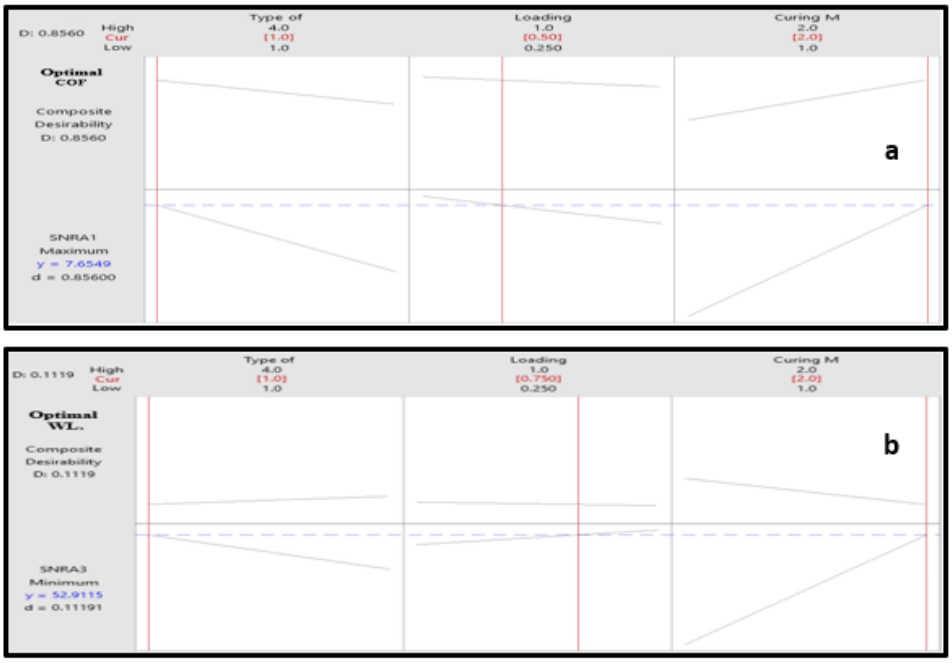

Fig. 5 Response Optimizer for COF and WL based on S/N ratio.

Tables 14 show that coefficient of friction, weight loss and hardness under consideration, the experimental and prediction responses are extremely similar. Based on S/N ratio response, a comparable degree of agreement is shown. Absolute error for COF, weight loss and hardness were calculated as 1.62 %, 0.46 % and 0.12 %, respectively. From these values for both the outputs, it appears that the resultant RSM model can accurately estimate the coefficient of friction, weight loss and hardness.

Table 14 Results of the prediction and experiment for S/N ratios values

Coefficient of friction			
	Prediction	Experiment	Absolut error %
Coefficient of friction S/N ratio (dB)	7.657	7.535	1.62 %
Weight loss			
Weight loss S/N ratio (dB)	52.91	53.152	0.46 %
Hardness			
Hardness S/N ratio (dB)	38.45	38.403	0.12 %

Response surface methodology

RSM is a common statistical method for formulating an approximate mathematical relationship between independent variables such as the type of filler, loading and curing method and the dependent variables (the main coefficient of friction, weight loss and hardness) for modelling, simulation, and optimization. The RSM works with identifying a region matching the ideal or ideal solution and encompasses the response(s) of a system for a variety of factor levels. First-order equations can be used as a strategy to mathematically connect the response to the factors. The pure linear system scarcely captures the true behavior of parameters in a complex system, where several factors interact to impact the output. In this view, it is preferable to represent the pertinent connection using the quadratic response function as indicated in Eq. 3.

$$Y = \beta_0 + \sum_{i=1}^{k} \beta_i X_i + \sum_{i=1}^{k} \beta_{ii} X_i^2 + \sum_{1 \le i \le j}^{k} \beta_{ij} X_i X_j + \varepsilon \quad (3)$$

where the input variable is xi, the dependent variable is X, the fixed term is βo, and the coefficients of the linear, quadratic, and cross-product terms are βi, βii, and βij, respectively.

A mathematical framework for the coefficient of friction has been constructed utilizing the S/N ratio in Eq. (4). Figure 6 exhibits that the average percentage efficiency is 94.68%, while the model deviation varies from 0.85% to 12.14%, located at runs 3 and 12, respectively.

$$\text{COF}_{S/N} = 6.505 - 0.14 \times \text{Type of filler} - 0.23 \times \text{Loading} + 0.703 \times \text{Curing method} \quad (4)$$

A weight loss mathematical model has been constructed according to the S/N ratio in Eq. (5). Figure 6 shows that the average percentage accuracy is 97.25%, whereas the

model deviation varies from 0.46% to 13.47%, preferably at runs 3 and 6, respectively.

$$Wl_{S/N} = 48.52 - 0.226 \times \text{Type of filler} + 0.39 \times \text{Loading} + 2.16 \times \text{Curing method} \quad (5)$$

A mathematical framework for hardness has been constructed utilizing the S/N ratio in Eq. (6). The model deviance ranges from 0.0033% to 0.349% (at run number 15 and 10 respectively), whereas the average percentage accuracy is 99.89%.

$$\text{Hardness}_{S/N} = 38.159 + 0.0499 \times \text{Type of filler} - 0.0003 \times \text{Loading} + 0.0454 \times \text{Curing method} \quad (6)$$

However, The graphs of COF and WL generated by the RSM model are illustrated in Figs. 6, 7 respectively. While the effect of parameters studied on the predicted COF is shown in Fig. 8.

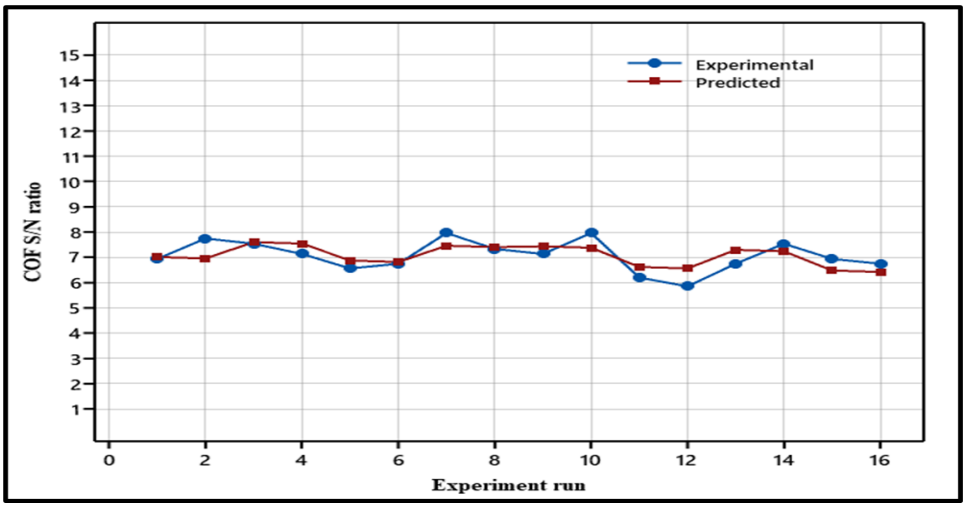

Fig. 6 Measured vs. predicted S/N ratio response (COF).

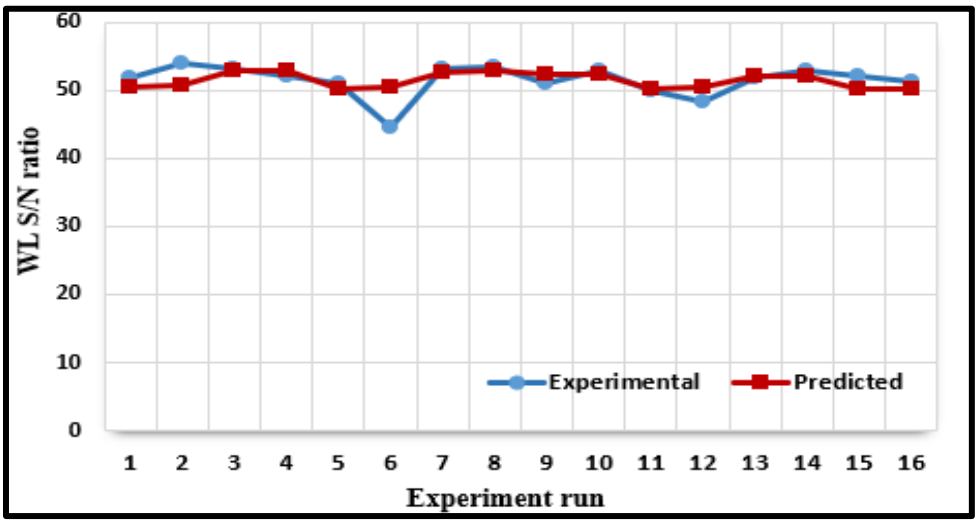

Fig. 7 Measured vs. predicted S/N ratio response (WL).

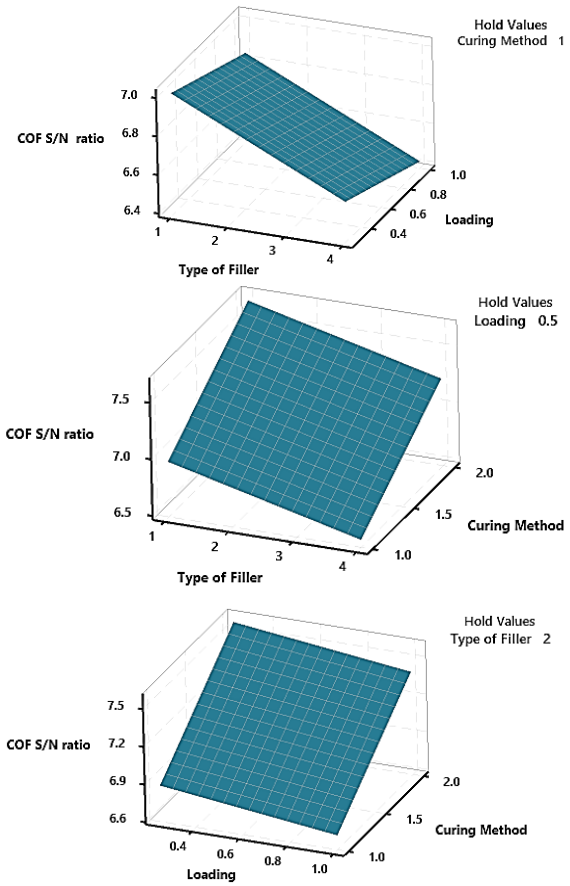

Fig. 8 Effect of parameters studied on the predicted COF.

CONCLUSIONS

This study utilized Taguchi's orthogonal array to optimize friction coefficient, weight loss and hardness. From the experimental findings, the following conclusions were derived:

1. Types of filler and curing method are the significant variables affecting COF.

2. The optimum conditions obtained from Taguchi method for optimizing COF is Type of filler of GN followed by Loading of 0.5 N and Curing method of heat cure.

3.According to Taguchi optimization results, the best WL are produced by Type of filler of GN followed by Loading of 0.75N and Curing method of heat cure the weight loss is attained.

4. The curing method contributes the most (33.75%), followed by type of filler (22.09%), and loading (10.25%), which makes up the least amount of the ideal Hardness, according to the ANOVA.

5. The validation of RSM models reveals that the mean percentage variation in the Coefficient of friction value is 5.32 %, the weight loss is 2.75%, and the hardness is 0.11 %.

6. Comparative analysis between experimental and predicted results demonstrated superior performance of RSM models.

7. The RSM model for Coefficient of friction achieved an impressive correlation

coefficient (R2) of 0.9468. Similarly, the model for weight loss yielded a correlation coefficient (R2) of 0.9725 and the model for hardness a correlation coefficient (R2) of 0.9989.

8. Multi-objective optimization using the desirability function enabled us to identify optimal parameters, resulting in an optimal Coefficient of friction at type of filler =GN., loading = 0.5 N and curing method = heat cure.

REFERENCES

1. Eyad M. A., Ali W. Y. and Nabhan A., "Wear Behavior of Cervical Fusion Plates Fabricated from Polyethylene Reinforced by Kevlar and Carbon Fibers", EGTRIB Vol 18, pp. 8–17 ,(2021).

2. Nabhan A., Taha M., Ibrahim A. M. M. and Ameer A. K., "Role of hybrid nanofiller GNPs/Al2O3 on enhancing the mechanical and tribological performance of HDPE composite", Sci Rep Vol.13, (2023).

3. Eyad M. A., Ali W. Y. and Nabhan A., "Mechanical Properties of cervical Fusion plates fabricated from Polyethylene reinforced by Kevlar and Carbon Fibers", KGK-Kautschuk Gummi Kunststoffe, Vol. 74, pp. 42–47, (2021).

4. Nabhan, A., Rashed, A. "Study of wear and friction behavior of HDPE-composite filled by CNTs. KGK Kautschuk Gummi Kunststoffe , Vol. 73, pp.27–38,(2020).

5. Zidan S., Silikas N., Al-Nasrawi S., Haider J., Alshabib A., Alshame A., and Yates, J.,"Chemical characterization of silanised zirconia nanoparticles and their effects on the properties of PMMA-zirconia nanocomposites", Materials , Vol. 14, pp.3212 ,(2021).

6. Patel V., Joshi U. and Joshi A. "Investigating the Effect of Hydroxyl Functionalized MWCNT on the Mechanical Properties of PMMA-Based Polymer Nanocomposites", Current Nanomaterials Vol. 8, pp.162–174, (2023).

7. Fouly A., Nabhan A. , and Badran A. , "Mechanical and Tribological Characteristics of PMMA Reinforced by Natural Materials", Egypt J Chem Vol.,65, pp1–2,(2022).

8. Gad M. M., Fouda S. M., Al-Harbi F. A., Näpänkangas R. and Raustia A.," PMMA denture base material enhancement: a review of fiber, filler, and nanofiller addition", Int J Nanomedicine Vol.12, No.3801,(2017).

9. Gad M. M. and Abualsaud R. "Behavior of PMMA denture base materials containing titanium dioxide nanoparticles: A literature review", Int J Biomater, (2019).

10. Dowding P. J. and Vincent B., "Suspension polymerisation to form polymer beads",Colloids Surf A Physicochem Eng Asp Vol.161, pp 259–269, (2000).

11. Moreno-Maldonado V., Acosta-Torres L. S., Barceló-Santana F. H., Vanegas-Lancón R. D., Plata-Rodríguez M. E., and Castano V. M.,"Fiber-reinforced nanopigmented poly (methyl methacrylate) as improved denture base", J Appl Polym Sci Vol.126,pp.289–296, (2012).

12. Acosta-Torres, L. S., López-Marín, L. M., Nunez-Anita, R. E., Hernández-Padrón, G. and Castaño," V. M. Biocompatible metal-oxide nanoparticles: Nanotechnology improvement of conventional prosthetic acrylic resins", J Nanomater,Vol.2011, No.941561, (2011).

13. Acosta-Torres L. S., Arenas M. C., Nuñez-Anita R. E., Barceló-Santana F. H., Álvarez-Gayosso C. A., Palacios-Alquisira J., and Castaño V. M., "Nanopigmented acrylic resin cured indistinctively by water bath or microwave energy for dentures", J Nanomater Vol.2014, No.198572, (2014).
14. H asratiningsih Z., Cahyanto A., Takarini V., Karlina E., Djustiana N., Febrida R. and Purwasasmita, B. S. "Basic properties of PMMA reinforced using ceramics particles of ZrO2-Al2O3-SiO2 coated with two types of coupling agents", Key Eng Mater Vol.696, pp.93–98,(2016).
15. Meshref A. A., Mazen A. A., El-Giushi M. A. and Ali W. Y., "Friction behavior of hybrid composites filled by titanium dioxide nanoparticles", Journal of the Egyptian Society of Tribology Vol.14, pp40–50, (2017).
16. Meshref A. A., Mazen A. A., El-Giushi M. A. & Ali W. Y., "Effect of Curing Process of Dental Nanocomposite Resin on Shore Hardness", Journal of the Egyptian Society of Tribology,Vol.13, pp.25–37, (2016).
17. Farhan F. K., Kadhim B. B., Ablawa B. D. and Shakir W. A. "Wear and friction characteristics of TiO_2–ZnO/PMMA nanocomposites", European Journal of Engineering and Technology Research, Vol2,pp. 6–9,(2017).
18. Salahuddin N., El-Kemary M. and Ibrahim E. "Reinforcement of polymethyl methacrylate denture base resin with ZnO nanostructures", Int J Appl Ceram Technol, Vol.15, pp.448–459,(2018).
19. Jagger D. C., Harrison A. and Jandt K. D. "The reinforcement of dentures", J Oral Rehabil ,Vol 26,pp.185–194 (1999).
20. Alshabib A., Silikas N. and Watts D. C."Properties of model E-glass fiber composites with varying matrix monomer ratios", Dental Materials, Vol 40, pp.441–450,(2024).
21. AminoroayaA., Neisiany R. E., Khorasani S. N., Panahi P., Das O., Madry H. and Ramakrishna, S."A review of dental composites: Challenges, chemistry aspects, filler influences, and future insights", Compos B Eng ,Vol. 216, No.108852 ,(2021).
22. Bocalon A. C., Mita D., Narumyia I., Shouha P., Xavier T. A., and Braga R. R. "Replacement of glass particles by multidirectional short glass fibers in experimental composites: Effects on degree of conversion, mechanical properties and polymerization shrinkage", Dental Materials, Vol.32, pp.e204–e210,(2016).
23. Borges A. L., Münchow E. A., de Oliveira Souza A. C., Yoshida T., Vallittu P. K., and Bottino, M. C. "Effect of random/aligned nylon-6/MWCNT fibers on dental resin composite reinforcement", J Mech Behavior Biomed Mater, Vol.48,pp. 134–144, (2015).
24. Ameer A. K., Mousa M. O. and Ali W. Y. "Tribological behaviour of poly-methyl methacrylate reinforced by multi-walled carbon nanotubes. KGK-Kautschuk Gummi Kunststoffe, Vol. 71,pp.40–46,(2018).
25. Wang R., Tao J., Yu B. and Dai L. "Characterization of multiwalled carbon nanotube-polymethyl methacrylate composite resins as denture base materials", J Prosthet Dent,Vol.111,pp.318–326,(2014).
26. Salih S. I., Oleiwi J. K. and Mohamed A. S., "Investigation of mechanical properties of PMMA composite reinforced with different types of natural powders", ARPN Journal of Engineering and Applied Sciences Vol.13, pp.8889–8900,(2018).

27. Rashed A. and Nabhan A. "Influence of adding nano graphene and hybrid SiO_2-TiO_2 nano particles on tribological characteristics of polymethyl methacrylate (PMMA) ", KGK-Kautschuk Gummi Kunststoffe, Vol.71, pp.32–37 ,(2018).
28. Salam M. A., Alsultany F. H., Al-Bermany E., Sabri M. M., Abdali K., and Ahmed, N. M " Impact of graphene oxide nanosheets and polymethyl methacrylate on nano/hybrid-based restoration dental filler composites: ultrasound behavior and antibacterial activity", J Ultrasound ,pp.1–20,(2024).
29. Abdu H. M., Tahaa S. M., Wazeer A., Abd El-Mageed A. M. and Mahmoud M. M."Application of Taguchi Method and Response Surface Methodology on Machining Parameters of Al MMCs 6063-TiO_2", Jordan J ournal of Mechanical & Industrial Engineering ,Vol.17, (2023).
30. Mansour H., Abo hashima H. & Elkhouly H. I. "Integrating between Taguchi methodology and boosted decision trees machine learning: a case study in enhancing quality electrical conductor manufacturing", Jordan Journal of Mechanical & Industrial Engineering ,Vol.18, (2024).
31. Divya G. S., Suresha B., Somashekar H. M. and Jamadar I. M. "Dynamic mechanical analysis and optimization of hybrid carbon-epoxy composites wear using Taguchi method", Tribology in industry, Vol.43,No.298 ,(2021).
32. Roy, R. K. A Primer on the Taguchi Method. (Society of manufacturing engineers, 2010).
33. Pervez H., Mozumder M. S. and Mourad A.-H. I. "Optimization of injection molding parameters for HDPE/TiO_2 nanocomposites fabrication with multiple performance characteristics using the Taguchi method and grey relational analysis", Materials, Vol. 9, No.710, (2016).
34. Natrayan L., Kumar P. A., Kaliappan S., Sekar S., Patil P. P., Velmurugan G. and Gurmesa M. D.,"Optimization of graphene nanofiller addition on the mechanical and adsorption properties of woven banana/polyester hybrid nanocomposites by Grey-Taguchi method", Adsorption Science & Technology, Vol.2022,No.1856828 ,(2022).
35. Řehoř J., Fulemová J., Kutlwašer J., Gombár M., Harničárová M., Kušnerová M. and Zatloukal, T. " ANOVA analysis for estimating the accuracy and surface roughness of precisely drilled holes of steel 42CrMo4 QT", The International Journal of Advanced Manufacturing Technology, Vol.126, pp.675–695, (2023).